Geometric and Hydrodynamic Modelling and Fluid-structural Relationships in the Southeastern Athabasca Basin and Significance for Uranium Mineralization

Zenghua Li[1], Guoxiang Chi[1], Kathryn M. Bethune[1], Sean A. Bosman[2] and Colin D. Card[2]

1. Department of Geology, University of Regina, Regina, Saskatchewan, S4S 0A2

2. Saskatchewan Geological Survey, Saskatchewan Ministry of the Economy, Regina, Saskatchewan, S4P 2H9

Abstract

Unconformity-type uranium deposits in the Athabasca Basin are spatially associated with reactivated basement faults intersecting the unconformity surface. However, questions such as what special factors focused fluid flow along and within fault zones, and why some faults are more fertile than others, are still unclear. This study aims to tackle these questions through examination of the southeastern Athabasca Basin. First, a basement structural map was compiled based on basement geophysical signatures, which shows three dominant sets of faults trending NE, NW, and NNW. A 3D model of the sub-Athabasca unconformity was constructed with GoCAD® using publicly available geological and drill-hole data, revealing a number of dominantly NE-trending ridges and valleys. These unconformity topographic features are interpreted to be the products of the combined action of three main factors: 1) pre-Athabasca group ductile faulting and alteration; 2) differential weathering and erosion; and 3) post-Athabasca reactivation of pre-existing, graphite-rich ductile shear zones. The basin-scale numerical modelling of hydrodynamics indicates that fluid pressures in the Athabasca Basin were close to hydrostatic throughout its sedimentary history, and that thermal convection cells may have been well developed in the lower part of the basin, particularly below the Wolverine Point Formation aquitard. The modeling results also show that individual convection cells are less than 2 km, implying that individual mineralization centres, if controlled by thermal convection, may be spaced at just a few kilometers. Local-scale numerical modelling of fluid flow indicates that the location and spacing of basement faults influence thermally-driven fluid convection. In a model with an isolated fault, the fault coincides with an upwelling plume. In the case of two faults, the faults may coincide with upwelling flow or alternatively be centrally located below convection cells, depending on fault spacing. In the latter case, fluid may flow into and out of individual fault zones. Modelling of fluid-flow in response to mechanical compression suggests that fluid migrates up the fault during compression, and that the models with the most shallowly dipping fault and those with offset on the fault have slightly greater flow rates than the other models. The various relationships between fluid-flow and faults can explain why some faults are more favourable for fluid flow than others, which may be potentially used to evaluate whether a given structure has the potential to host mineralization.

Introduction

Unconformity-type uranium deposits are the largest known high-grade deposits of uranium in the world. A common feature is their close spatial association with reactivated basement faults intersecting the unconformity surface (Jefferson et al., 2007). However, significant gaps remain in our understanding of these deposits. One important question concerns what special factors focused fluid flow at specific sites within the basin, especially along fault zones and within wider structural zones, and why some faults are more prospective than others. While recent studies advocate that fluid flow was either downward into basement fault zones ("ingress" deposits), or upward and outward from such zones ("egress" deposits), and that these systems were potentially linked (Jefferson et al., 2007), the dynamics involved remain poorly understood. It has been proposed that the fluid flow related to uranium mineralization in the Athabasca Basin was driven by thermally induced fluid convection (Raffensperger and Garven, 1995), but little is known about the sizes of the convection cells and how these may affect the localization of mineralization. There is also the question of whether ingress flow and egress flow were associated with alternating compressional and extensional stress fields, accompanied by fluid pressure fluctuation (Cui et al., 2012). Finding answers to these questions is of economic significance, because it will help to discriminate between fault-fluid-alteration/lithology combinations fertile for uranium mineralization and those that are less prospective.

This study focused on the southeastern Athabasca Basin, which hosts all of Canada's current producing unconformity-related uranium mines, to tackle these questions. First, a basement structural map was compiled in GoCAD® based on geophysical data (Card et al., 2010). This was subsequently combined with a 3D model of the unconformity surface constructed using drill-hole data (data from Geological Atlas of Saskatchewan) to illustrate the relationships between basement structures, the unconformity surface topography and uranium mineralization. The basin-scale hydrodynamic background was then analyzed based on fluid pressure modeling, which was used as the initial conditions for numerical modelling of heat and deformation related fluid flow. Simulations of thermal convection, with consideration of the influence of basement faults and their spacing on convection cells, and fluid flow in response to compressional stresses, taking into account different orientations of the faults, were carried out using FLAC3D® software. FLAC3D® is a finite difference code capable of simulating the interaction of fluid flow, tectonic deformation, and heat transport based on various material constitutive models (Itasca, 2012). Finally, the significance of the modelling results for localization of uranium deposits was examined. Some of the study results have been published (Li et al., 2013, 2014a and b; Chi et al., 2014), and more modelling is

Li, Z., Chi, G., Bethune, K.M., Bosman, S.A., and Card, C.D., 2015. Geometric and Hydrodynamic Modelling and Fluid-structural Relationships in the Southeastern Athabasca Basin and Significance for Uranium Mineralization, *in* Targeted Geoscience Initiative 4: unconformity-related uranium systems, (ed.) E.G. Potter and D.M. Wright; Geological Survey of Canada, Open File 7791, p. 103–114. doi:10.4095/295776

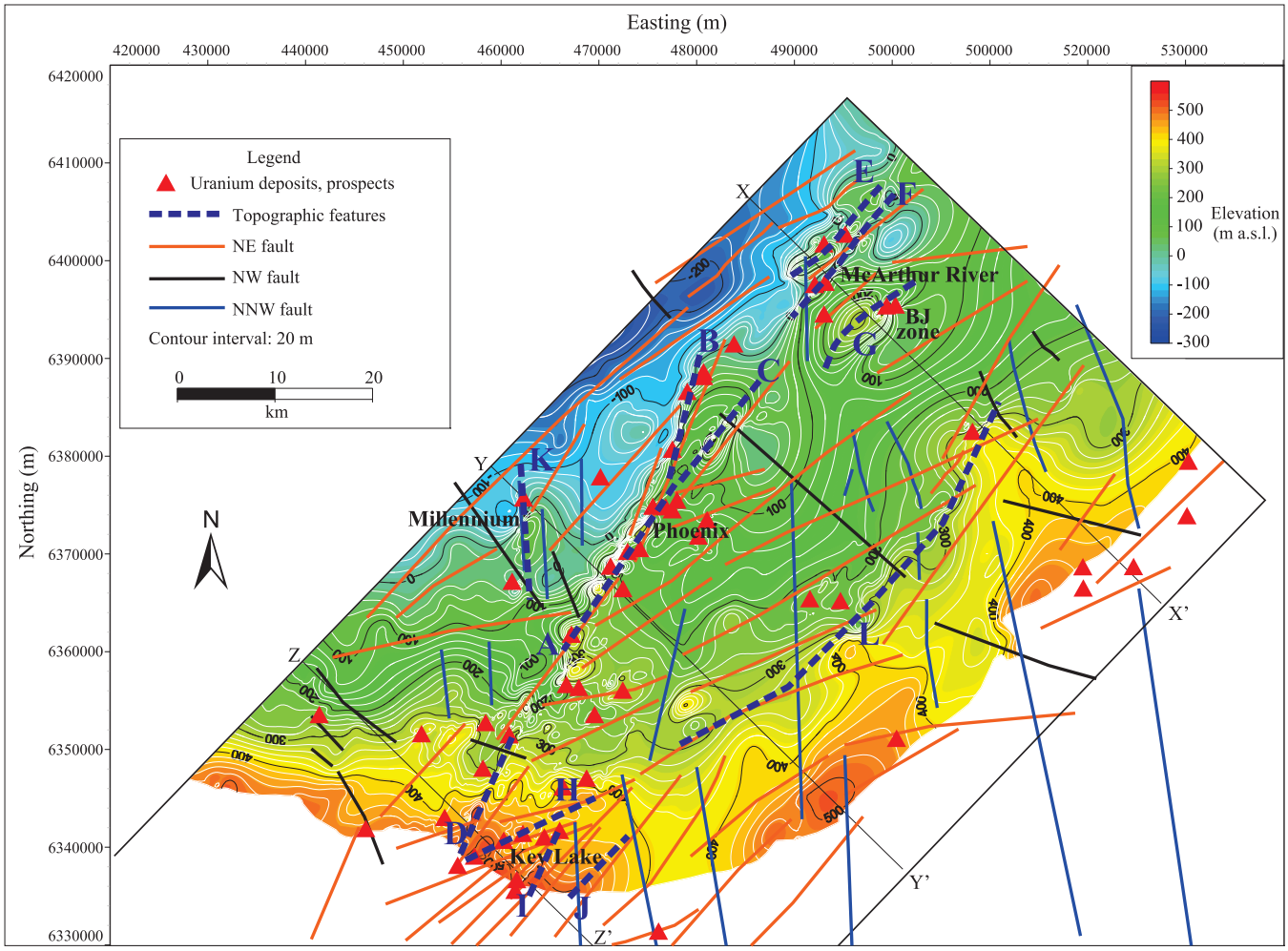

Figure 1. Contour maps showing the elevations of the sub-Athabasca unconformity in the study area. Faults, interpreted on the basis of aeromagnetic data (Card et al., 2010) are also superimposed on the contoured unconformity surface.

underway to further test the influence of fault dip angles, kinematics, spacing and networking on fluid flow, as well as the interaction between thermally-driven and deformation-driven flow.

Modelling results

Three-dimensional modelling of the unconformity surface of the southeastern Athabasca Basin

A 3D model of the southeastern Athabasca Basin was constructed to evaluate the spatial configuration of basement structures and the unconformity, as well as clay alteration patterns in relation to lithology and structures. The main purpose of this model was to determine where, when and how uranium-bearing fluids may have travelled (Li et al., 2013), which can then be used to guide subsequent fluid-flow modelling under different deformational and thermal conditions (Li et al., 2014b), as discussed in more detail in the sections below.

The 3D model highlights an approximately NE-trending zone of elevated topography of the unconformity surface associated with the Phoenix-McArthur River deposit trend, as well as a number of other prominent topographic features (Figs. 1 and 2). Several prominent ridges of metaquartzite proximal to faults along this trend (Earle and Sopuck, 1989), including those at the McArthur and Phoenix deposits (Marlatt et al., 1992; Kerr, 2010), were recognized. These topographic features can be explained through the combined action of three main factors: 1) pre-Athabasca group ductile faulting and alteration; 2) differential weathering and erosion; and 3) post-Athabasca fault reactivation, localized in pre-existing, graphite-rich ductile shear zones (e.g. Györfi et al., 2007; Jefferson et al., 2007; Ramaekers et al., 2007; Tourigny et al., 2007; Yeo et al., 2007).

Faults were identified using the basement geophysical signature, in combination with evidence of unconformity offset. Three dominant sets of faults, inferred to be sub-vertical, were identified on this basis: NE, NW, and NNW, in chronological order from oldest to youngest (Fig. 1). Nearly all the uranium deposits and prospects are associated with the NE-trending structures and adjacent unconformity topographic highs (Fig. 1). Regional clay anomalies documented in previous studies (Earle and Sopuck, 1989) are also broadly aligned with this dominant trend (Li et al., 2013).

It is inferred that pre-Athabasca faulting likely con-

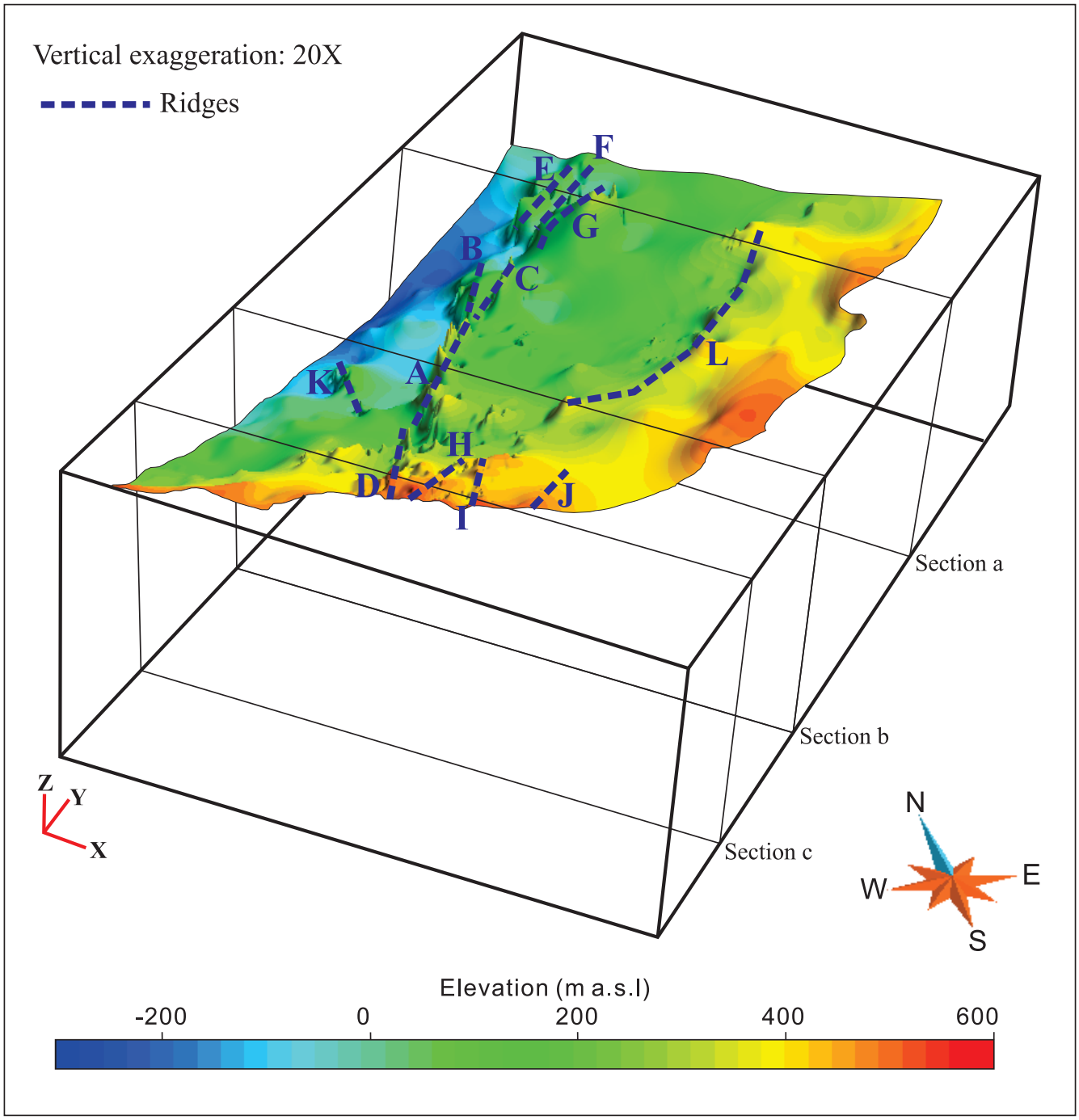

Figure 2. 3D view of the sub-Athabasca unconformity in the study area. Prominent basement ridges are highlighted.

tributed in a substantial way to shaping the paleo-topography of the unconformity surface, which in turn controlled early sedimentation in the basin. Some of the faults were reactivated during and after deposition of the Athabasca Group, further modifying the topography of the unconformity surface. Both the primary unconformity topography and post-Athabasca faulting may have played a role in fluid flow, controlling alteration patterns and uranium mineralization (e.g. Earle and Sopuck, 1989; Harvey and Bethune, 2007; Jefferson et al., 2007; Long, 2007).

Hydrodynamic background of the Athabasca Basin

In order to decipher the mechanisms of fluid flow responsible for uranium mineralization, it is important to understand the background hydrodynamic conditions and temperatures of the basin. These parameters also provide constraints on the initial and boundary conditions required for numerical modelling of fluid flow.

Recent numerical studies by Chi et al. (2013) confirmed that no significant fluid overpressure due to disequilibrium sediment compaction was developed in the basin during sed-

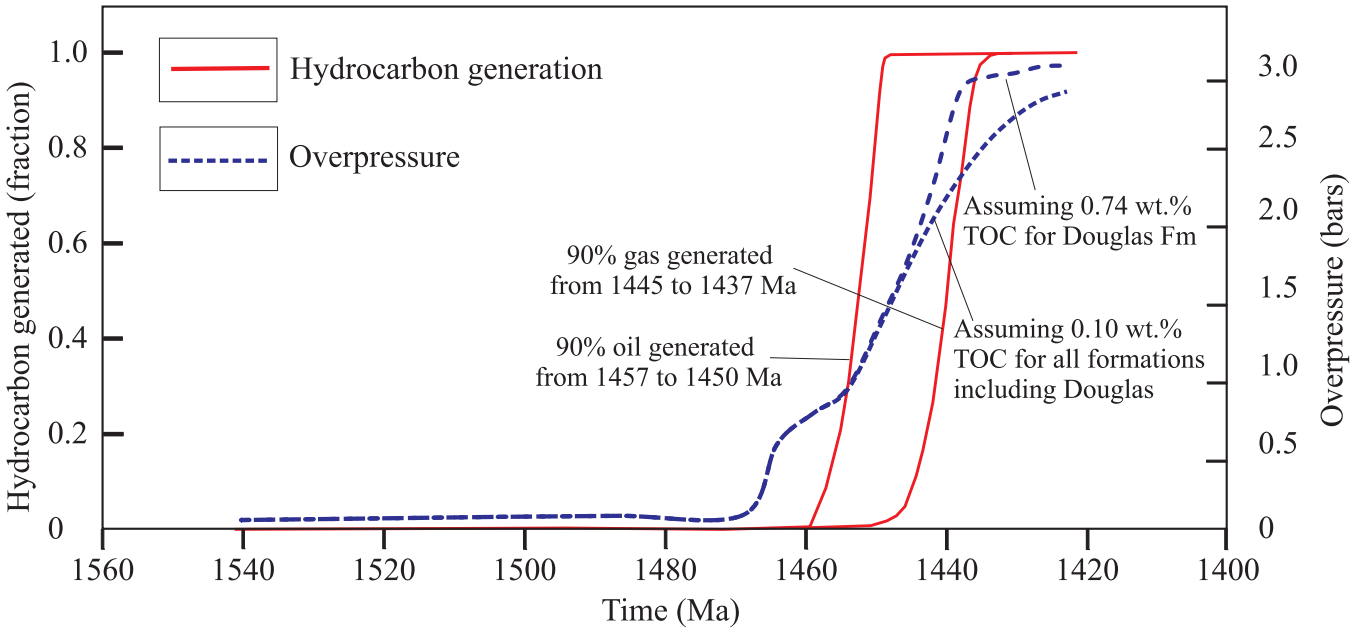

Figure 3. Numerical modeling results showing the time intervals of oil and gas generation in the Douglas Formation in the basin centre, and the evolution of fluid overpressure in the Douglas Formation in the basin centre, as compared to a model with 0.1 wt. % TOC (modified from Chi et al., 2014).

imentation. In other words, the fluid pressure within the basin was near the hydrostatic regime throughout its depositional history, i.e., from ca. 1740 to 1541 Ma (Rainbird et al., 2007). Fluid flow related to sediment compaction was very slow and the temperature profile was undisturbed, implying that if compaction-driven flow was responsible for mineralization, the sites of mineralization would not record thermal anomalies (Chi et al., 2013).

A complementary study was undertaken by Chi et al. (2014) to evaluate how hydrocarbon generation processes in the Douglas Formation, which contains total organic carbon (TOC) of up to 3.56 wt. % (Stasiuk et al., 2001), may have affected fluid overpressure development in the basin (Fig. 3). The authors reported that if each lithology is assigned a moderate permeability (the 'base model'), oil and gas generation processes contribute little to the development of fluid overpressure, and fluid pressure in the basin was close to hydrostatic regardless of whether or not hydrocarbon generation in the Douglas Formation is included in the modelling. However, if the permeability of each lithology is assigned a value one order of magnitude lower than in the base model, significant fluid overpressures are developed in the eroded strata in the upper part of the model. In the base model, oil generated in the Douglas Formation may migrate downward, driven by an overpressure zone situated above the Douglas Formation, but gas migrates upward. In the low-permeability model, however, the overpressures developed above the Douglas Formation are so high that both oil and gas generated in the Douglas Formation will migrate downward. The numerical modelling therefore indicates that, under certain conditions, it would be hydrodynamically possible for oil and gas generated in the ca. 1541 Ma Douglas Formation to migrate to the base of the basin and reach the sites of the unconformity-related uranium deposits, which formed at ca. 1600 – 1500 Ma and 1460 – 1350 Ma, with significant remobilization events at ca. 1176 Ma, 900 Ma, and 300 Ma (Hoeve and Quirt, 1984; Cumming and Krstic, 1992; McGill et al., 1993; Kyser et al., 2000; Fayek et al., 2002; Alexandre et al., 2003; 2009; Creaser and Stasiuk, 2007).

The inference that fluid pressures in the Athabasca Basin were close to hydrostatic values throughout its history has important implications for further fluid flow models. Fluid flow driven by topographic relief and fluid convection driven by density variation are relatively easy to develop when the initial fluid-pressure system is near hydrostatic; strong fluid overpressure in the basin tends to suppress such fluid flow (Chi et al., 2013). This suggests that fluid flow driven by topographic relief (e.g. Alexandre and Kyser, 2012) or convection related to fluid density variation due to thermal gradients (e.g. Raffensperger and Garven, 1995) are both theoretically plausible.

Fluid convection due to geothermal gradients

In order to accurately address the question of how fluid behaved at a local scale and in relation to faulting, a basin-scale modeling of fluid convection is required. Such work has been done for the Athabasca Basin by Raffensperberg and Garven (1995), but the actual sizes of the individual convection cells and their relationship with the thicknesses of the strata remain unclear due to scaling factors. Therefore, we carried out a modeling of basin-scale thermal convection with a more realistic physical model, using FLAC3D® (Itasca, 2012).

The physical model is similar to that used by Chi et al. (2013), where the basin is divided into sedimentary formations and members, each with a different permeability (Fig. 4). Hydrostatic pressure and a thermal field with a gradient of 35°C/km were the initial conditions assigned to the sys-

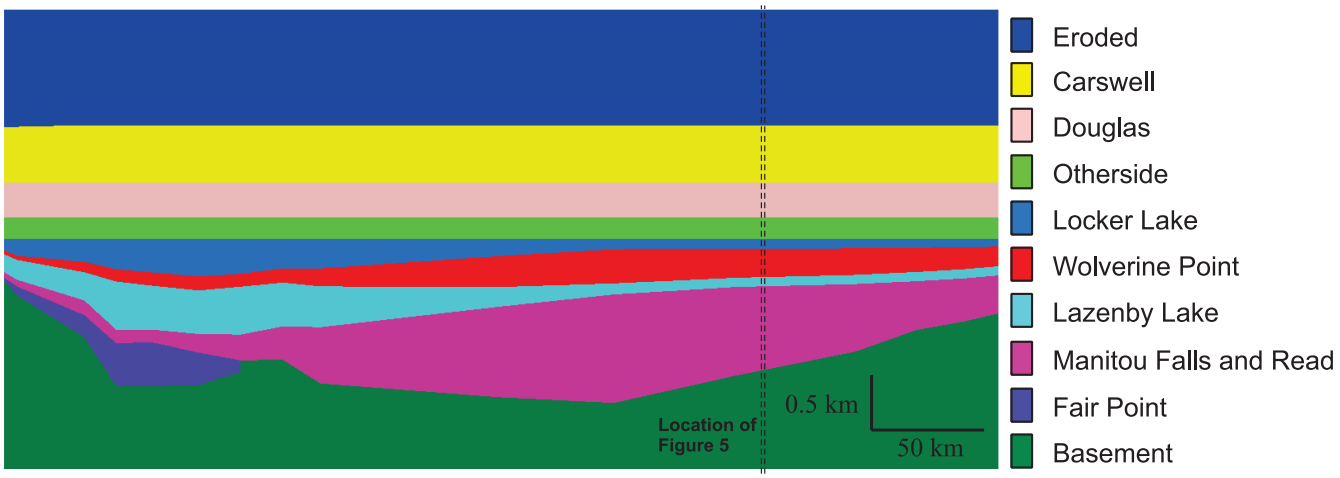

FIGURE 4. Sectional view of the geometric basin model developed for numerical modelling. Dashed lines show the location of Figure 5. Note vertical exaggeration.

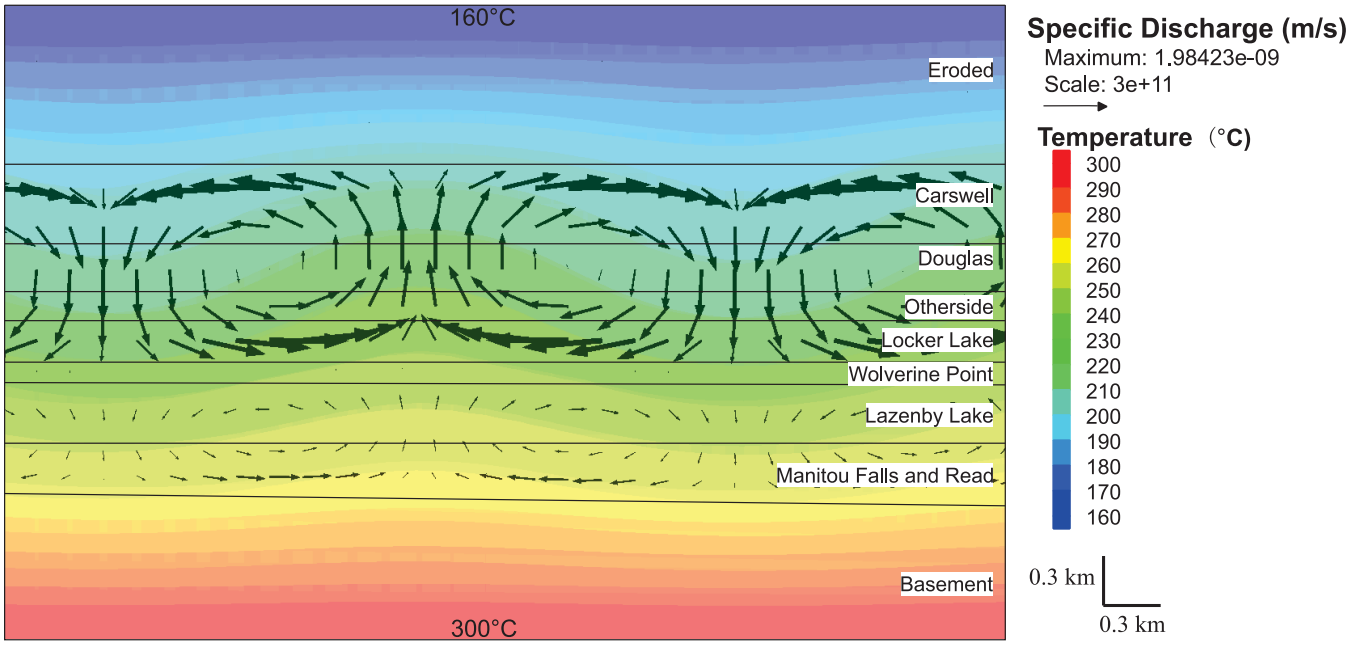

FIGURE 5. Numerical modelling results showing area of the basin outlined by the dash lines in Figure 4. Temperatures are indicated by colour-coded isotherms. Fluid-flow patterns are shown by streamlines, with arrows indicating fluid-flow directions and the size of the arrows reflecting flow rate.

tem. The upper boundary was open to fluid flow and the side and bottom boundaries were assumed to be impermeable to fluid flow. For heat transport, the temperature of the top and bottom boundaries was fixed based on a geothermal gradient of 35°C/km and surface temperature 20 °C. The two side boundaries were insulated to heat transport.

The numerical experiments suggest that when low permeability is assigned to the mudstone-rich Wolverine Point Formation aquitard (Jefferson et al., 2007; Ramaekers et al., 2007), thermal convection cells were developed in the lower part of the basin, particularly below the Wolverine Point Formation, as well as in the upper part of the basin (if high permeability is assumed for the strata now eroded) at geothermal gradients of 25 to 35 °C/km (Fig. 5). The results also show that the largest convection cells formed above the Wolverine Point Formation (Fig. 5). Changes to the assumed geothermal gradient do not modify the fluid flow patterns at the basin scale.

It is notable that the sizes of the convection cells are controlled by the thickness of the sandstone units when all other parameters are held constant; that is, larger thicknesses give rise to larger convection cells. A sensitivity study shows that convection cell size is also controlled by the permeability of the sandstone layers (i.e. higher permeability produces smaller cell sizes).

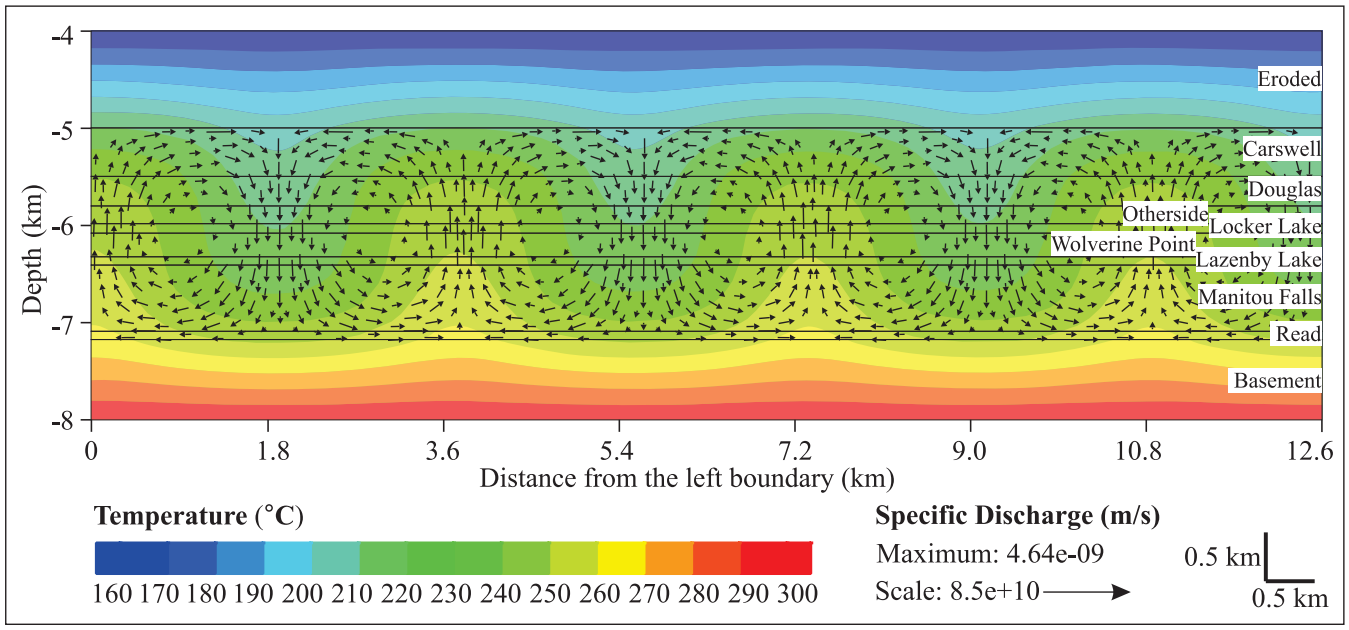

FIGURE 6. Numerical modelling results showing fluid-flow patterns without any faults.

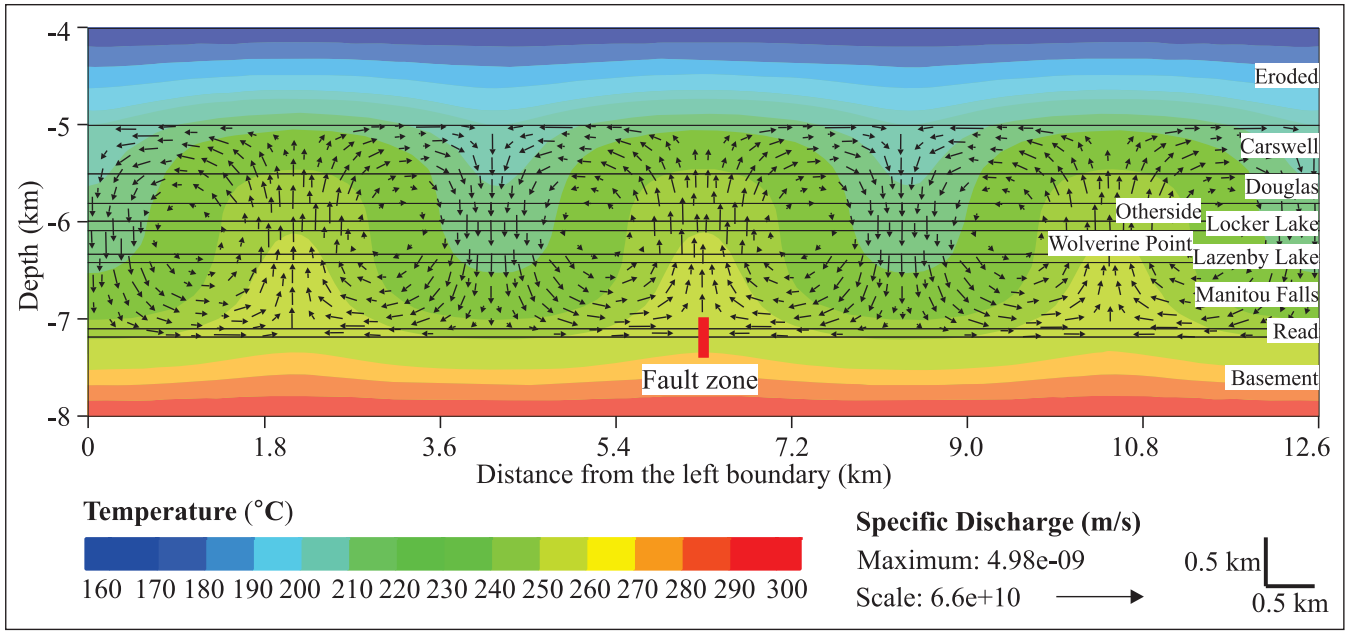

FIGURE 7. Numerical modelling results showing fluid-flow patterns associated with one fault in the centre.

Effects of basement faults on fluid convection cells

To better understand the effects of basement faults on fluid convection due to geothermal gradient, two scenarios were tested. The first scenario incorporated one vertical fault, whereas the second incorporated two vertical faults spaced at 1.8 km and 3.6 km, respectively. The model fault zone was 100 m wide by 400 m high and straddled the unconformity. At this stage of study, only the space and position of the fault zones are considered in the models; faults with different dip angles will be incorporated in the next step. The boundary and initial conditions are the same as those employed in basin-scale model.

For the models with one fault, the fault controls the initial position of the convection cells, i.e. it coincides with the upwelling plume of two adjacent cells (Figs. 6–8). When the fault is moved from the centre to the left for half the size of a convection cell, the upwelling plume shifts from the centre to left accordingly (Figs. 7 and 8).

Like the one-fault model, the faults in the two-fault model also control the initial position of the convection cells, each fault coinciding with an upwelling plume in the beginning. Depending on the spacing of the two faults, however, the final results are different after the models reach steady state. When the spacing of the two faults is equal to the size

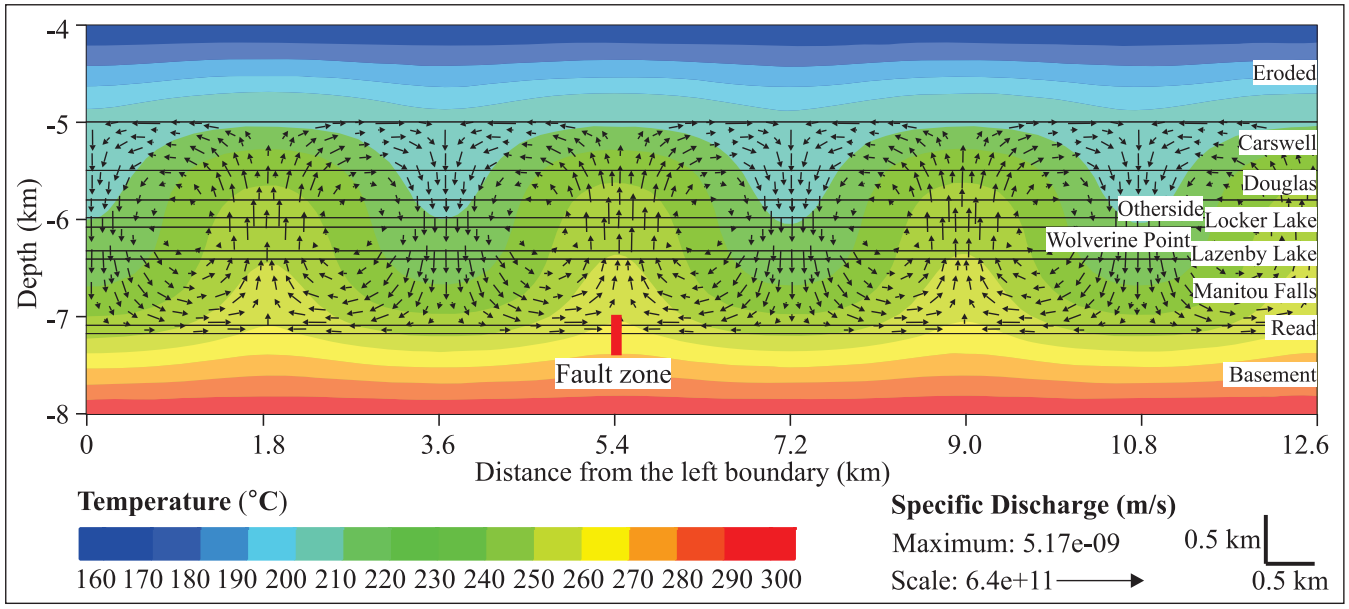

Figure 8. Numerical modelling results showing fluid-flow patterns associated with one fault situated to the left relative to the model shown in Figure 7.

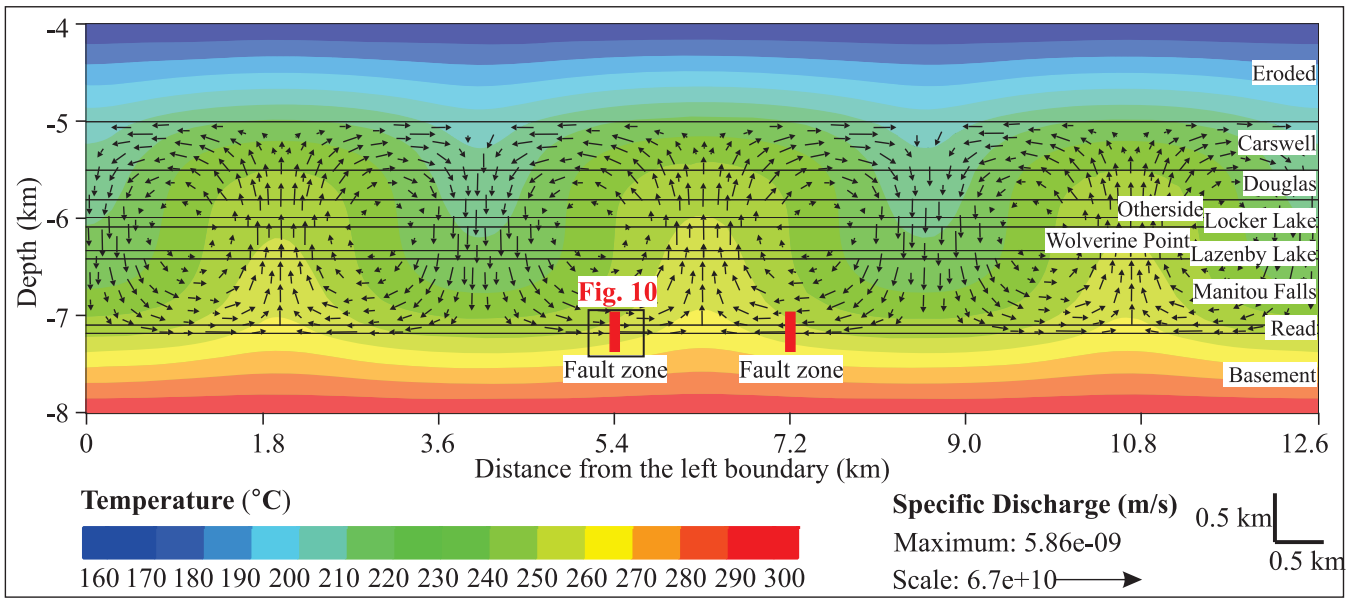

Figure 9. Numerical modelling results showing fluid-flow patterns associated with two faults, with spacing one size of the convection cell in the non-fault model.

of the convection cells in the one-fault model (i.e. 1.8 km), the unstable and weak cells developed at the early stage are destroyed by neighbouring cells after the model reaches a stable state. As a result, the size of the convection cells corresponding to the fault zones is increased; furthermore, neither of the faults coincides with an upwelling or downwelling stream (Fig. 9). Unlike the models with one fault, fluid can penetrate into basement along the fault zone through thermal convection, flowing down one side and up on the other side, depending on the flow direction and where the fault zone is located (Fig. 10). However, when the spacing of the faults is twice as large as the size of the convection cell in the one-fault model (i.e. 3.6 km), the total number and size of the cells remain the same as in the one-fault model, and no fluid penetrates into the basement along fault zone (Fig. 11).

Relationship between fluid-flow and mechanical compression

Preliminary numerical modelling of fluid flow in response to mechanical compression using the 3D model of the Athabasca Basin described above as a guide has been conducted with FLAC3D®. Four scenarios incorporating reverse faults with different dip angles have been tested (Li

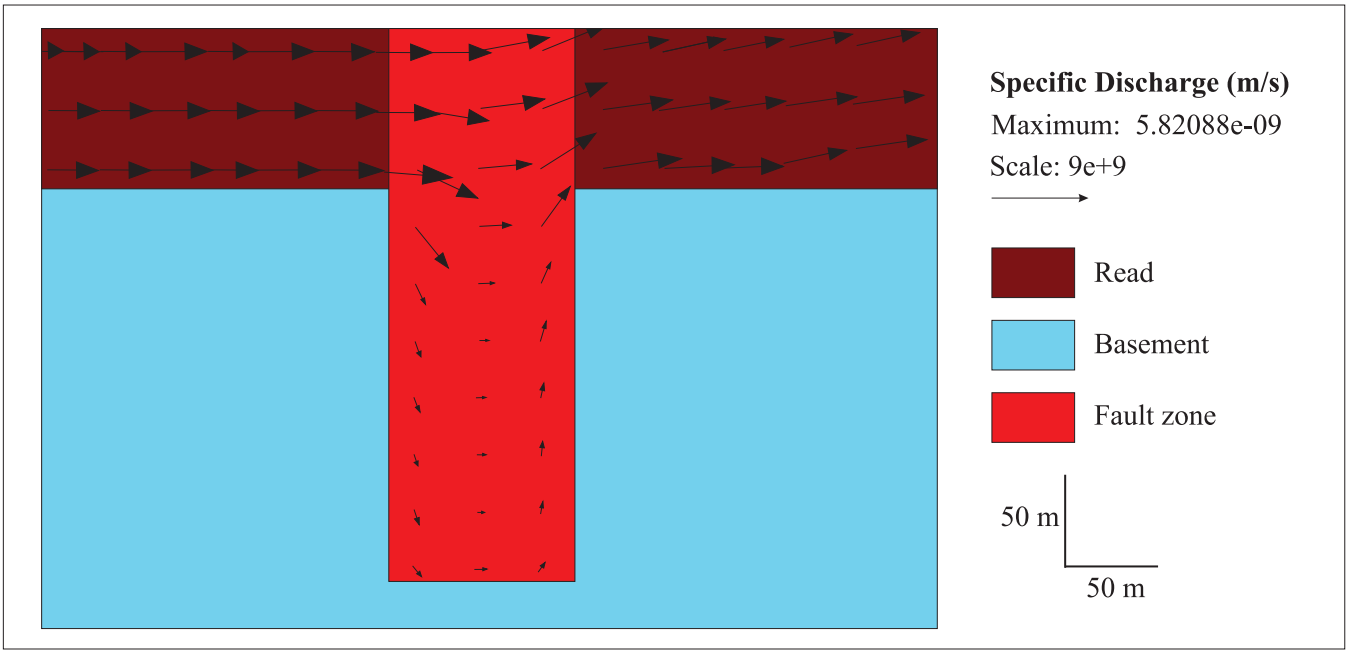

FIGURE 10. Expanded view of the left fault in figure 9, illustrating fluid penetration into the basement rocks along the fault zone.

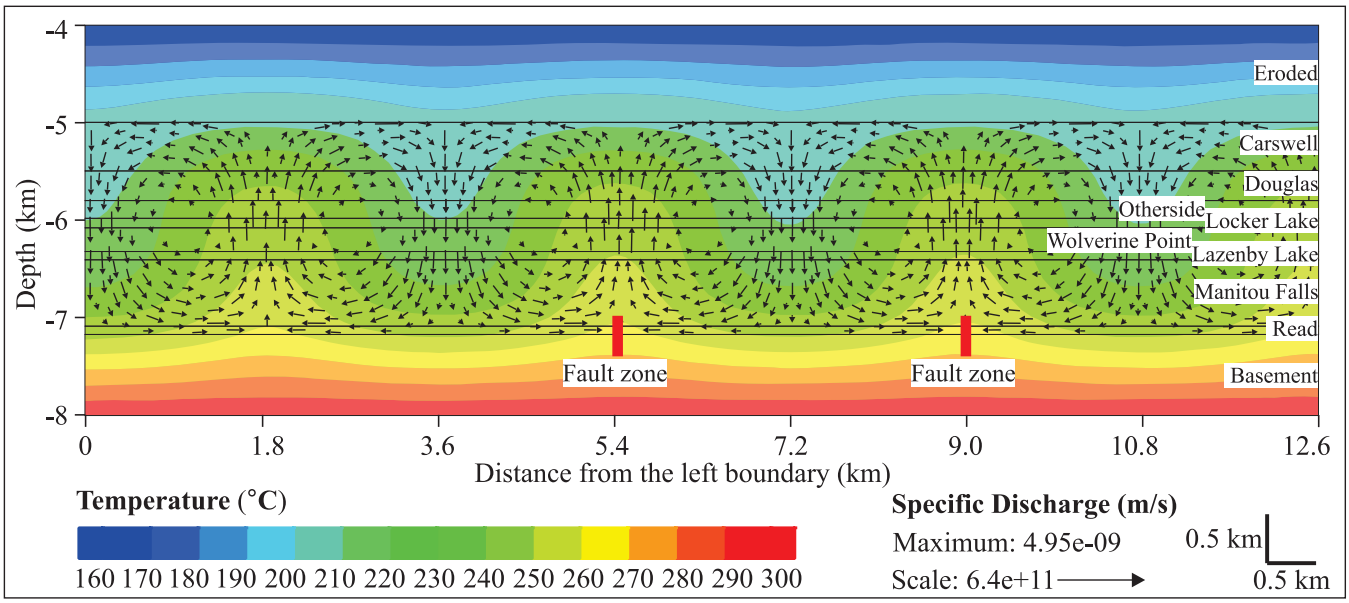

FIGURE 11. Numerical modelling results showing fluid-flow patterns associated with two faults, with spacing at double the size of the convection cell in the non-fault model.

et al., 2014b).

An initial model is shown in Figure 12. This model portrays a relatively simple geological situation based on aggregate thickness of stratotypes (Ramaekers et al., 2007) and estimates of eroded units, where basement rocks are overlain by 2 km of more permeable sandstone representing the basal Athabasca Group, which are in turn overlain by 4 km of eroded strata. A 300 m wide northwest-dipping fault (with a dip angle of 45°) transects the unconformity but does not offset it; the fault is inferred to extend one km above and below the unconformity (Figs. 12 and 13b). The other two scenarios have the same model parameters, except for dip angles of 30° and 60°, respectively (Figs. 13a and 13c), whereas the last scenario tests the effect of offset of the unconformity on fluid flow during compression (Fig. 13d). All the models are subjected to NW-SE horizontal shortening to simulate the tectonic compression. The top of the model was free to deform in both the vertical and horizontal directions to reflect the fact that topography changes during tectonic deformation. The base was fixed vertically, but was free to move horizontally to account for tectonic deformation.

The modelling results show that during compressive

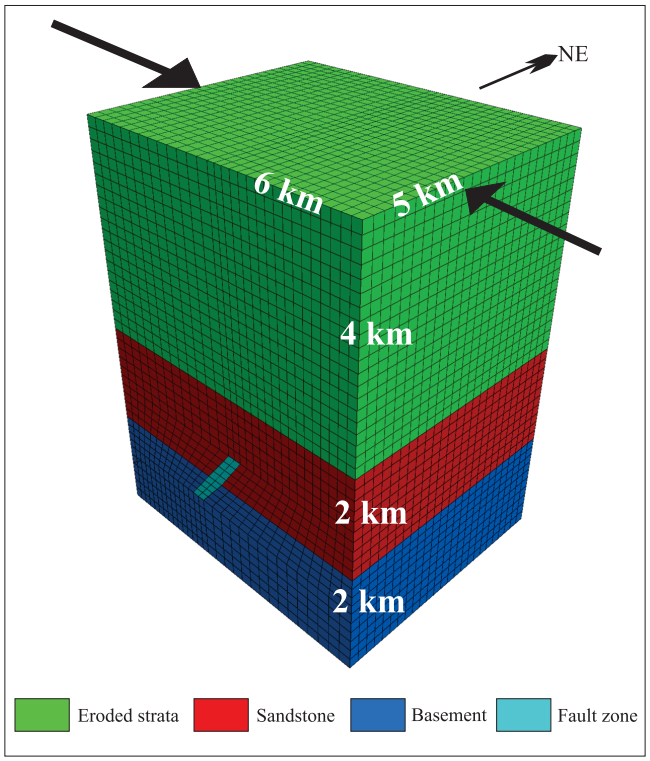

Figure 12. 3D view of the initial model used for numerical modelling of fluid flow in response to mechanical compression.

deformation, fluid migrates up the fault (Fig. 13), which is consistent with the results of Cui et al. (2012). This is due to the rapid increase of pore pressure in the low-permeability basement, the fault zone being an area of dilation and low fluid pressure relative to the surrounding basement rocks. The results of different models incorporating faults with different dip angles show that flow patterns are generally the same amongst the models. However, the model with the most shallowly dipping fault shows slightly greater flow rates than the other models. This is due to the fact that the shallowly dipping fault undergoes more dilation because its orientation is closest to the direction of the maximum principal stress (horizontal and SE-NW). The model with offset on the fault also shows a slightly greater flow rate – suggesting an increase in dilation controlled by differences in properties between units. The fault zones represent the most significant loci of shear strain in all models. As expected, the dip of the fault also strongly controls the orientation of the high strain zone, which propagates into the sandstone (Fig. 13).

Summary and implications for exploration

A 3D model of the sub-Athabasca unconformity has been constructed using publicly available geological and drillhole data. Faults have been identified primarily using basement geophysical signatures, and also from publically available data (Card et al., 2010). Three dominant sets of faults, inferred to be sub-vertical, were identified on this basis: NE, NW, and NNW, in chronological order from oldest to youngest. Numerous dominantly northeast-trending ridges and valleys have been identified in the sub-Athabasca unconformity surface. These features are interpreted to be the products of the combined action of three main factors: 1) pre-Athabasca group ductile faulting and alteration; 2) differential weathering and erosion; and 3) post-Athabasca fault reactivation, localized in pre-existing, graphite-rich ductile shear zones (Györfi et al., 2007; Jefferson et al., 2007; Ramaekers et al., 2007; Tourigny et al., 2007; Yeo et al., 2007). Although unconformity topographic features immediately adjacent to uranium deposits may be positive (ridges) or negative (valleys) (e.g. Harvey and Bethune, 2007; Kerr, 2010; Marlatt et al., 1992), they are all related to structures (Jefferson et al., 2007). These topographic features as well as structures are also spatially associated with the regional distribution of EM conductors, clay alteration patterns of the overlying Athabasca Group (e.g. Earle and Sopuck, 1989) and uranium enrichment (Jefferson et al., 2007). This implies that basement paleotopography may have played an important role in controlling and perhaps localizing fluid flow related to mineralization (e.g. Harvey and Bethune, 2007), and therefore accurate modelling of the unconformity surface may be used to define fertile areas of uranium deposits.

The basin-scale numerical modelling results indicate that fluid pressures in the Athabasca Basin were close to hydrostatic values throughout its development, and that thermal convection cells may have been well developed in the lower part of the basin, particularly below the Wolverine Point Formation aquitard, as well as in the upper part of the basin (if high permeability is assumed for the strata now eroded). These results, when compared with basin-wide geochemical data that indicate significant differences in chemical composition between the Wolverine Point Formation and the underlying strata (Chu et al., 2015; Wright and Potter, 2014), suggest that the highly permeable lower part of the Athabasca Basin experienced extensive chemical changes due to large-scale fluid circulation. These results also indicate that if fluid convection is limited to the high-permeability strata below the Wolverine Point Formation, individual convection cells are likely less than 2 km, although the convection cell size may be increased if the upper part of the basement has permeability comparable to those of the covering strata. If individual convection cells are considered as potential mineralization centres, the spacing between these centres may be just a few kilometers. This is of interest for uranium exploration within individual districts.

Local-scale numerical modelling of fluid flow indicates that the location and spacing of basement faults influences thermally driven fluid convection. Fault controls the initial position of the convection, and isolated faults generally coincide with upwelling flow, but they may also be located within a convection cell under certain configurations of fault spacing. In the latter case, fluid may flow into and out of the same fault zone. Modelling results of fluid flow due to mechanical compression suggest that fluid migrates up the fault during compression, and that the model with the most shallowly dipping fault and the model with fault offset of the unconformity show slightly greater flow rates than the other models. Collectively, these results further support the empirical model that faults crosscutting the unconformity played

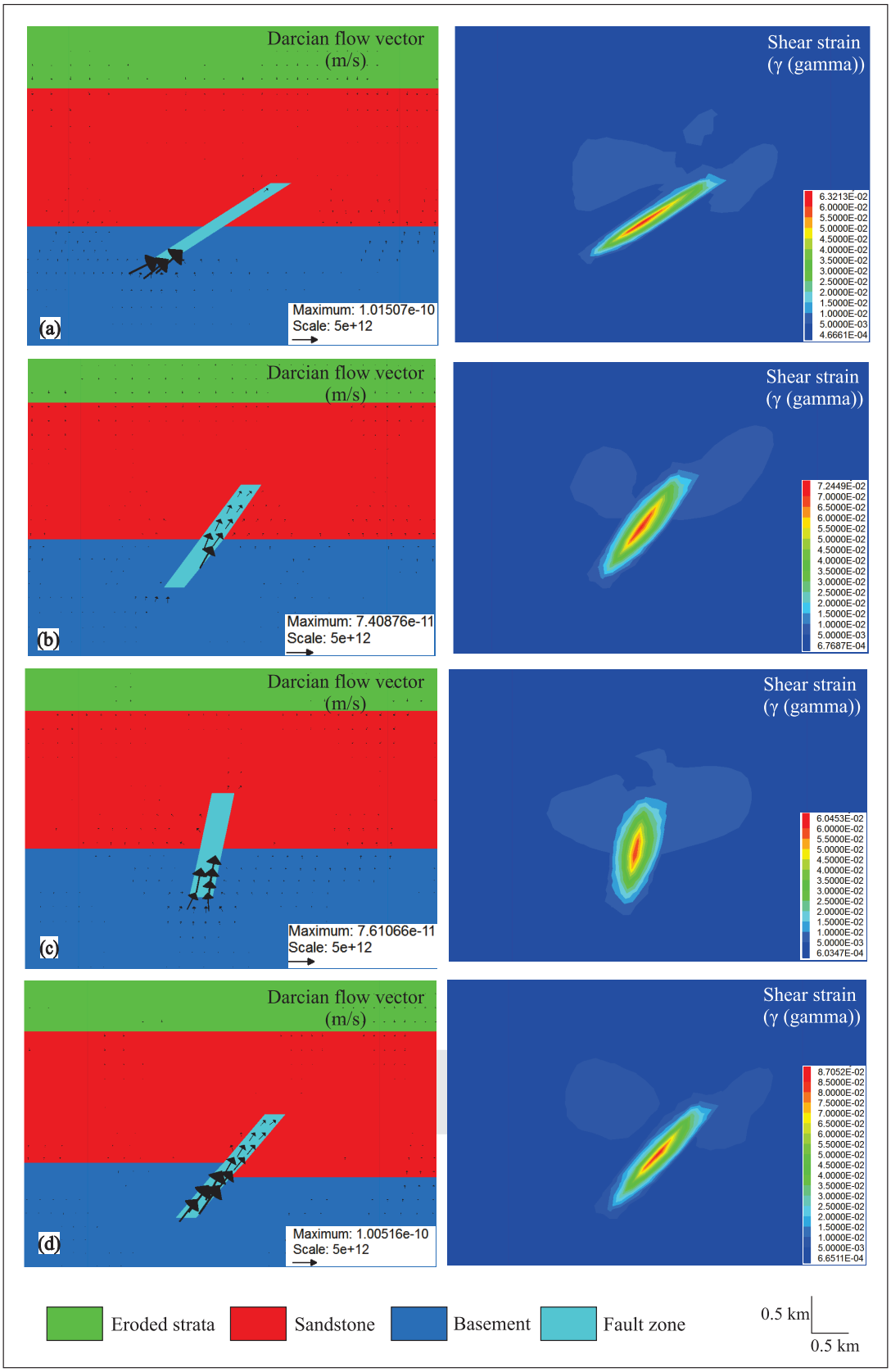

FIGURE 13. Sectional plots of fluid flow vectors (left) and shear strain development (right) for each model after 0.1% shortening. Black arrows indicate the direction of fluid flow and length of arrows indicates magnitude of Darcian fluid-flow (m/s). Shear strain is recorded by γ (gamma) values.

an important role in localizing fluid flow and uranium mineralization, either through controlling convection cell location or providing fluid flow driving forces. The various relationships between convection cells and faults (position and spacing), in addition to other constraints such as fault kinetics and orientations, may explain why some faults are more favourable for fluid-flow than others. All these factors are potentially important in determining whether a given structure may host mineralization.

Acknowledgments

Funding for this research was provided by the Targeted Geoscience Initiative 4 (TGI-4) uranium ore systems project, through a grant to K.M. Bethune and G. Chi, and in part by a NSERC-Discovery grant (to G. Chi). Access to the GoCAD licenses were kindly provided by the Saskatchewan Geological Survey. Denison Mines Corp. is thanked for logistical support and access to drill cores. The authors also wish to thank Jianwen Yang and Eric G. Potter for editorial comments and critical reviews.

References

Alexandre, P., and Kyser, T.K., 2012. Modeling of the fluid flow involved in the formation of Athabasca Basin unconformity-type uranium deposits; Joint annual meeting of the Geological Association of Canada - Mineralogical Association of Canada, Abstracts, v. 35, p. 3.

Alexandre, P., Kyser, T.K., and Polito, P., 2003. Geochronology of the Paleoproterozoic basement-hosted unconformity-type uranium deposits in northern Saskatchewan, Canada; Uranium Geochemistry 2003, International Conference, Proceedings, p. 37–40.

Alexandre, P., Kyser, T.K., Thomas, D., Polito, P., and Marlat, J., 2009. Geochronology of unconformity-related uranium deposits in the Athabasca Basin, Saskatchewan, Canada and their integration in the evolution of the basin; Mineralium Deposita, v. 44, p. 41–59.

Card, C.D., Bosman, S.A., Slimmon, W.L., Delaney, G., Heath, P., Gouthas, G., and Fairclough, M., 2010. Enhanced geophysical images and multiscale edge (worm) analysis for the Athabasca region; Sask. Ministry of Energy and Resources, Open File 2010-46.

Chi, G., Bosman, S., and Card, C., 2013. Numerical modeling of fluid pressure regime in the Athabasca basin and implications for fluid flow models related to the unconformity-type uranium mineralization; Journal of Geochemical Exploration, v. 125, p. 8–19.

Chi, G., Li, Z., and Bethune, K.M., 2014. Numerical modeling of hydrocarbon generation in the Douglas Formation of the Athabasca basin (Canada) and implications for unconformity-related uranium mineralization; Journal of Geochemical Exploration, v. 144, Part A, p. 37–48.

Chu, H., Chi, G., Bosman, S., and Card, C. 2015. Diagenetic and geochemical studies of sandstones from drill core DV10-001 in the Athabasca basin, Canada, and implications for uranium mineralization; Journal of Geochemical Exploration, v. 148, p. 206–230.

Creaser, R.A., and Stasiuk, L.D., 2007. Depositional age of the Douglas Formation, northern Saskatchewan, determined by Re-Os geochronology; in EXTECH IV: Geology and Uranium EXploration TECHnology of the Proterozoic Athabasca Basin, Saskatchewan and Alberta, (ed.) C.W. Jefferson and G. Delaney; Geological Survey of Canada, Bulletin 588, p. 341–346.

Cui, T., Yang, J.W., and Samson, I.M., 2012. Tectonic deformation and fluid flow: implications for the formation of unconformity-related uranium deposits; Economic Geology, v. 107, p. 147–163.

Cumming, G.L., and Krstic, D., 1992. The age of unconformity-associated uranium mineralization in the Athabasca Basin, northern Saskatchewan; Canadian Journal of Earth Sciences, v. 29, p. 1623–1639.

Earle, S.A.M., and Sopuck, V.J., 1989. Regional lithogeochemistry of the eastern part of the Athabasca Basin uranium province, Saskatchewan, Canada; in Uranium Resources and Geology of North America; International Atomic Energy Agency, TECDOC-500, p. 263–296.

Fayek, M., Kyser, T.K., and Riciputi, L.R., 2002. U and Pb isotope analysis of uranium minerals by ion microprobe and the geochronology of the McArthur River and Sue Zone uranium deposits, Saskatchewan, Canada; The Canadian Mineralogist, v. 40, p. 1553–1569.

Györfi, I., Hajnal, Z., White, D.J., Takács, E., Reilkoff, B., Annesley, I.R., Powell, B., and Koch, R., 2007. High-resolution seismic survey from the McArthur River region: contributions to mapping of the complex P2 uranium ore zone, Athabasca Basin, Saskatchewan; in EXTECH IV: Geology and Uranium Exploration TECHnology of the Proterozoic Athabasca Basin, Saskatchewan and Alberta, (ed.) C.W. Jefferson and G. Delaney; Geological Survey of Canada, Bulletin 588, p. 397–412.

Harvey, S.E., and Bethune, K.M., 2007. Context of the Deilmann orebody, Key Lake mine, Saskatchewan; in EXTECH IV: Geology and Uranium Exploration TECHnology of the Proterozoic Athabasca Basin, Saskatchewan and Alberta, (ed.) C.W. Jefferson and G. Delaney; Geological Survey of Canada, Bulletin 588, p. 249–266.

Hoeve, J., and Quirt, D.H., 1984. Mineralization and host rock alteration in relation to clay mineral diagenesis and evolution of the middle-Proterozoic, Athabasca Basin, northern Saskatchewan, Canada; Saskatchewan Research Council, SRC Technical Report 187, 187 p.

Itasca, 2012. FLAC3D: Fast Lagrangian Analysis of Continua in 3 Dimensions, User's Guide, version 5.0; Itasca Consulting Group Inc., Minnesota.

Jefferson, C., Thomas, D., Gandhi, S., Ramaekers, P., Delaney, G., Brisbin, D., Cutts, C., Portella, P., and Olson, R., 2007. Unconformity-associated uranium deposits of the Athabasca Basin, Saskatchewan and Alberta; in EXTECH IV: Geology and Uranium Exploration TECHnology of the Proterozoic Athabasca Basin, Saskatchewan and Alberta, (ed.) C.W. Jefferson and G. Delaney; Geological Survey of Canada, Bulletin 588, p. 23–67

Kerr, W.C., 2010. The discovery of the Phoenix Deposit; a new high-grade, Athabasca Basin unconformity-type uranium deposit, Saskatchewan, Canada; Society of Economic Geologists Special Publications, v.15, p. 703–728.

Kyser, K., Hiatt, E., Renac, C., Durocher, K., Holk, G., and Deckart, K., 2000. Diagenetic fluids in Paleo- and Mesoproterozoic sedimentary basins and their implications for long protracted fluid histories; in Fluids and Basin Evolution, (ed.) T.K. Kyser; Mineralogical Association of Canada Short Course Series, v. 28, p. 225–262.

Li, Z., Bethune, K.M., Chi, G., Bosman, S.A., and Card, C.D., 2013. Preliminary 3D modelling and structural interpretation of southeastern Athabasca Basin; Geological Survey of Canada, Open File 7426.

Li, Z., Bethune, K.M., Chi, G., Card, C.D., and Bosman, S.A., 2014a. Topographic features of the sub-Athabasca Group unconformity surface in southeastern Athabasca Basin and its relationship to uranium ore deposits; Joint annual meeting of the Geological Association of Canada - Mineralogical Association of Canada, Abstracts v.37, p. 162.

Li, Z., Chi, G., Bethune, K.M., Bosman, S., and Card, C.D., 2014b. Preliminary 3D geomodelling and simulation of coupled fluid flow and compressional deformation in the Athabasca Basin; Geological Survey of Canada, Open File 7612, one sheet.

Long, D.G.F. 2007. Topographic influences on the sedimentology of the Manitou Falls Formation, eastern Athabasca Basin, Saskatchewan; in EXTECH IV: Geology and Uranium Exploration TECHnology of the Proterozoic Athabasca Basin, Saskatchewan and Alberta, (ed.) C.W. Jefferson and G. Delaney; Geological Survey of Canada, Bulletin 588, p. 267–280.

Marlatt, J., McGill, B., Matthews, R., Sopuck, V., and Pollock, G., 1992. The discovery of the McArthur River uranium deposit, Saskatchewan, Canada; in New Developments in Uranium Exploration, Resources, Production and Demand; International Atomic Energy Agency and the Nuclear Energy Agency of the Organization for Economic Cooperation Development, IAEA-TECDOC-650, p. 118–127.

McGill, B.D., Marlatt, J.L., Matthews, R.B., Sopuck, V.J., Homeniuk, L.A., and Hubregtse, J.J., 1993. The P2 north uranium deposit, Saskatchewan, Canada; Exploration and Mining Geology, v. 2, p. 321–331.

Raffensperger, J.P., and Garven, G., 1995. The formation of unconformity-type uranium ore-deposits. 1. Coupled groundwater-flow and heat-

transport modeling; American Journal of Science, v. 295, p. 581–636.

Rainbird, R.H., Stern, R.A., Rayner, N., and Jefferson, C.W., 2007. Age, provenance, and regional correlation of the Athabasca Group, Saskatchewan and Alberta, constrained by igneous and detrital zircon geochronology; in EXTECH IV: Geology and Uranium Exploration TECHnology of the Proterozoic Athabasca Basin, Saskatchewan and Alberta, (ed.) C.W. Jefferson and G. Delaney; Geological Survey of Canada, Bulletin 588, p. 193–209.

Ramaekers, P., Jefferson, C.W., Yeo, G.M., Collier, B., Long, D.G.F., Drever, G., Mchardy, S., Jiricka, D., Cutts, C., Wheatley, K., Catuneanu, O., and Bernier, S., 2007. Revised geological map and stratigraphy of the Athabasca Group, Saskatchewan and Alberta; in EXTECH IV: Geology and Uranium Exploration TECHnology of the Proterozoic Athabasca Basin, Saskatchewan and Alberta, (ed.) C.W. Jefferson and G. Delaney; Geological Survey of Canada, Bulletin 588,. 155–192.

Stasiuk, L.D., Fowler, M.G., Jiricka, D., Mossisson, D., Sopuck, V., Wheatley, K., Wilson, N.S., and Zaluski, G., 2001. Preliminary investigation into organic petrology and organic geochemistry of Proterozoic Douglas Formation shales and Athabasca Group sandstones distal and proximal to uranium mineralization, Athabasca Basin, Saskatchewan; in Summary of Investigations 2001, Saskatchewan Geological Survey, Saskatchewan Energy and Mines, Miscellaneous Report 2001-4.2, vol. 2, p. 224–239.

Tourigny, G., Quirt, D.H., Wilson, N.S.F., Wilson, S., Breton, G., and Portella, P., 2007. Geological and structural features of the Sue C uranium deposit, McClean Lake area, Saskatchewan; in EXTECH IV: Geology and Uranium Exploration TECHnology of the Proterozoic Athabasca Basin, Saskatchewan and Alberta, (ed.) C.W. Jefferson and G. Delaney; Geological Survey of Canada, Bulletin 588, p. 229–247.

Wright, D.M. and Potter, E.G., 2014. Regional surface rock geochemistry, Athabasca Basin. Saskatchewan; Geological Survey of Canada, Open File 7614, 33 pages, doi:10.4095/293915.

Yeo, G.M., and Delaney, G., 2007. The Wollaston Supergroup, stratigraphy and metallogeny of a Paleoproterozoic Wilson cycle in the Trans-Hudson Orogen, Saskatchewan; in EXTECH IV: Geology and Uranium Exploration TECHnology of the Proterozoic Athabasca Basin, Saskatchewan and Alberta, (ed.) C.W. Jefferson and G. Delaney; Geological Survey of Canada, Bulletin 588, p. 89–118.